საქართველოს მეცნიერებათა ეროვნული აკადემიის მოამბე, ტ. 5, №1, 2011
BULLETIN OF THE GEORGIAN NATIONAL ACADEMY OF SCIENCES, vol. 5, no. 1, 2011

Human and Animal Physiology

Electrophysiological and Morphological Properties of Units in the Lateral Central Nucleus of the Amygdala

Gogi Todua

P. Anokhin Institute of Higher Nervous Activity and Neurophysiology, Russian Academy of Sciences, Moscow; I. Beritashvili Institute of Physiology, Tbilisi

(Presented by Academy Member Tengiz Oniani)

ABSTRACT. Intracellular recordings from units of the lateral part of central amygdaloid nucleus [CeL] were performed under urethane anesthesia in cat. A total of 32 neurons were recorded. Their membrane properties and firing patterns were analyzed with intracellular current injections. The mean input resistance and time constant, measured in 13 neurons were 29.4±5MΩ and 22.2÷3.4 ms respectively. Based on their firing properties in response to 100-400 ms depolarizing current injection, neurons were classified into two types: adapting and regular spiking. Adapting cells were further subdivided into fast adapting and slow adapting types according to their firing frequency adaptation. 9 electrophysiologically identified neurons were stained with an intracellular injection of biocytin and were analyzed morphologically. Their somata were oval or spindle in shape and the mean size was 18x13.4 μm. Putative integrative role of CeL neurons, in relation to the intrinsic and extrinsic connections is discussed. © *2011 Bull. Georg. Natl. Acad. Sci.*

Key words: *amygdaloid complex, central nucleus, membrane properties, current pulse, input resistance.*

Central nucleus of the amygdala [CN] is an important region, which integrates sensory information, provided by cortical, amygdaloid, thalamic and brainstem areas to elaborate coordinated autonomic, endocrine and somatic responses. Not so long ago it was an obscure region of the amygdala, that attracted relatively little scientific interest. Today it is one of the most heavily studied area of the amygdala. CN is subdivided into four sectors: capsular, lateral, intermediate and medial. Tract tracing studies have revealed that these subdivisions have extensive intranuclear and extranuclear connectivity [1-3].

Amygdaloid complex is involved in emotional responses, especially in fear and fear conditioning [4-6]. Much data suggest that the lateral nucleus [LN] is the sensory gateway into the amygdala. It receives major cortical and thalamic sensory pathways and sends efferents to other amygdaloid nuclei [7, 8], whereas the medial part of the central nucleus [CeM] is the mean output station for conditioning fear responses. It has substantial projections to the hypothalamus, bed nucleus of the stria terminalis and several nuclei in the midbrain, pons and medulla [9-11]. Projections to the brain stem are to three main areas: the periaqueductal gray, which leads to vocalization, startle analgesia and cardiovascular changes, the parabrachial nucleus which is involved in pain pathways, and the nucleus of solitary tract, which is connected with the vagal system. Discrete electrolytic lesion of the LN disrupts somatosensor and cardiac pressor conditioned responses to auditory conditioned stimuli [5]. Similarly, lesions of the CeM or its brainstem and hypothalamic targets abolish conditioned fear responses [12]. At present it is unclear how conditioned stimuli evoked activity is relayed from the LN to CeM. Indeed, the LN does not project to the CeM, but sends glutamatergic projections to the CeL[13], as well as to the basolateral and basomedial nuclei [14]. Output units of these structures could trans-

mit conditioned stimulus evoked activity to the CeM, because their axons form asymmetric synaptic contacts with the CeM neurons [15]. CeL, which forms the largest projection to the CeM, receives large extraamygdaloid inputs from both cortical and subcortical sources: the insular cortex, several thalamic nuclei, including the paraventricular nucleus, the mesencephalic dopaminergic centers and the parabrachial nucleus [16, 17] suggesting that it might also be a site of integration of inputs to the amygdaloid complex. Despite the importance of this region, the physiological and morphological properties of the different cell types in CeL are not as well characterized as those of cell types in the lateral and basal nuclei of the amygdala. The present experiments were designed to identify CeL cells, which send their axonal projections to CeM and to study the electrophysiological and morphological properties of these cells.

5 cats were used in experiments. They were anesthetized by intravenous injection of urethane (1.2 g/kg). Supplemental doses were injected intraperitoneally during the experiment. The animal was then mounthained on a stereotaxic instrument. Animals were then paralyzed with gallamine triethiodide (4 mg/kg) and artificially ventilated. Stability of recordings was ensured by cisternal drainage. Body temperature was maintained 36-37°C by means of heating pad. Stimulating and recording electrodes were inserted according to coordinates of the stereotaxic atlas of Jasper and Ajmone-Marsan [20]. Stainless steel bipolar electrodes (0.5 mm diameter, 0.5 mm tip separations) were implanted in the CeM (A11.5-12.5 L3-4 H -3,-4) to activate CeL units antidromically. Square pulses of 0.1ms duration and 6-20V intensity were used. Activity of CeL neurons was recorded with glass micropipettes filled with 2M potassium citrate. Coordinates used for recording electrodes were:A12.5-13, L2-3, H-2.5, -3.5). The resistance of these electrodes was of 15-30 MΩ. Impalements of neurons were considered acceptable when the membrane potential was at least –60mV and the spike amplitude >50mV. Signals from microelectrodes were filtered, amplified and displayed on an oscilloscope for visual observation and photography. The criteria for the antidromic responses were as follows: constant latency, faithful responses to high rates of stimulation (above 250 Hz), a short refractory period (usually of less than 2 ms.), no preceding prepotentials and collision with an orthodromic spike. The firing patterns and membrane properties of identified output units were studied with 100-400 ms. Pulse currents were injected through a bridge circuit (Axoclamp 2A). Spike threshold, defined as the membrane potential corresponding to the slope break point, was expressed as the mean membrane potential at which spontaneous action potentials were triggered. In cells that did not exhibit spontaneous firing the threshold was determined for the first spike, evoked by depolarizing intracellular current pulse. Spike amplitude was measured from threshold to peak and spike duration at half amplitude. The rheobase was measured as the lowest current intensity leading to spike discharge from resting potential (pulses of 400 ms. duration). To assess the input resistance of neurons we measured the average voltage response to the injection of hyperpolarizing current pulses of weak intensity (100 ms duration 0.3 nA 0.3 Hz) through recording electrode. Current-voltage relationship was established by injecting square-wave current pulses (100 ms duration) with increasing intensity. Voltage responses were measured at their peak deflection during and at the apparent steady-state 10ms before the offset of the current steps. The time constants were estimated from averages of typically 0.1 nA, 200 ms hyperpolarized pulses as the time necessary to reach 63% of the maximum voltage deflection.

Following electrophysiological analysis biocytin was injected iontophoretically with 2 nA of depolarizing current (300 ms. duration 1-2 Hz) for 2-10 min. At the end of experiments animals were deeply anesthetized with sodium pentobarbital (35 mg/kg) and perfused with buffered 7% formalin through the ascending aorta. Brains were dissected immediately and stored in 20% sucrose buffer solution overnight. Serial sagital sections of 60 μm in thickness were cut on a freezing microtome. The sections were processed with biotin-avidin complex to visualize the biocytin-injected neurons by horseradish peroxidase histochemical reaction [18]. The morphology of stained neurons was examined with light microscope and those thus selected were reconstructed with camera lucida drawings. The morphological parameters - the longer and shorter diameters of soma, the cell volume and the radius dendritic field were measured [19].

A total of 32 neurons projected to CeM were recorded from CeL in the present study. These cells had a stable resting membrane potential more negative than -60mV. The latency of antidromic spikes ranged from 0.6 to 1.8ms. and the mean conduction velocity was 1.2m/sec. Fig.1 displays examples of antidromic responses. These responses satisfied all criteria for antidromic activation. Unit responded to CeM stimulation with a stable latency of 1.1ms. [A]. The antidromic nature of responses was further verified by their colliding with orthodromic spikes [B]. Refractoriness of CeL neurons was studied by double shock technique. Examples are shown in C-E. At the time interval of 2.5 ms. between shocks the IS-SD inflection of the second spike became more prominent [C]. With 2 ms. interval the test SD spike was blocked, leaving only the IS

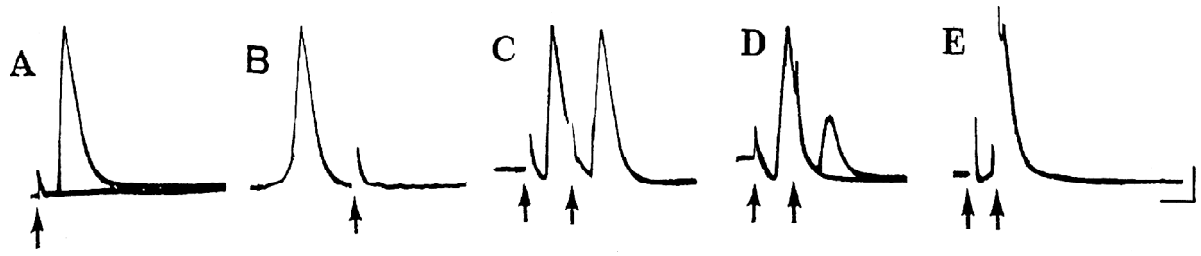

Fig. 1. Examples of antidromically evoked spikes of GL units to CeM stimulation. A. superposition of 5 raw traces showing the stability of the spike latency. B. collision of antidromic spike with action potential, elicited orthodromically. The antidromic spike collides with orthodromic action potential at an interval of 2.1 ms CDE. Responses to antidromic double stimulation of same neuron with interstimulus interval of 2.5; 2 and 1.6 ms. respectively. Time calibration 2 ms; Voltage calibration 20 mV.

spike [D]. At 1.6 ms. interval between shocks the IS component was also blocked.

Firing patterns of CeL units and their membrane properties were analyzed with intracellular current injection, through conventional bridge circuit. In population of 22 units firing properties in response to 100-400 ms. 0.1-0.5 nA depolarizing current injection were studied. Spike half amplitude duration ranged from 0.7 to 0.8ms. The mean rheobase was 0.27-0.37nA and firing threshold ranged from -44.6 to -51.8mV. Two mean classes of output cells were distinguished on the basis of their evoked firing pattern in response to intracellular prolonged depolarizing pulses: adapting and regular spiking cells. 18 of the recorded cells (81.8%) were classified as adapting cells. These cells were characterized by varying degrees of spike frequency adaptation, adapting cells were further classified as fast adapting and slow adapting according to the spike frequency adaptation during their evoked discharge. Fast adapting cells to application of high and moderate intensity depolarizing current pulses responded with an initial train of spikes (3-7) followed by a depolarizing plateau (Fig. 2AB). Careful grading of injected current intensity near the threshold evoked single spikes, even with current pulses of several milliseconds. The duration of the train of spikes was slightly lengthened by increasing the depolarizing current intensity and its maximal mean duration was 53±21 ms. At all current intensities within the train the interspike intervals progressively increased (Fig. 2C) and the spike amplitude showed slight variations.

In the second group of adapting cells named slow

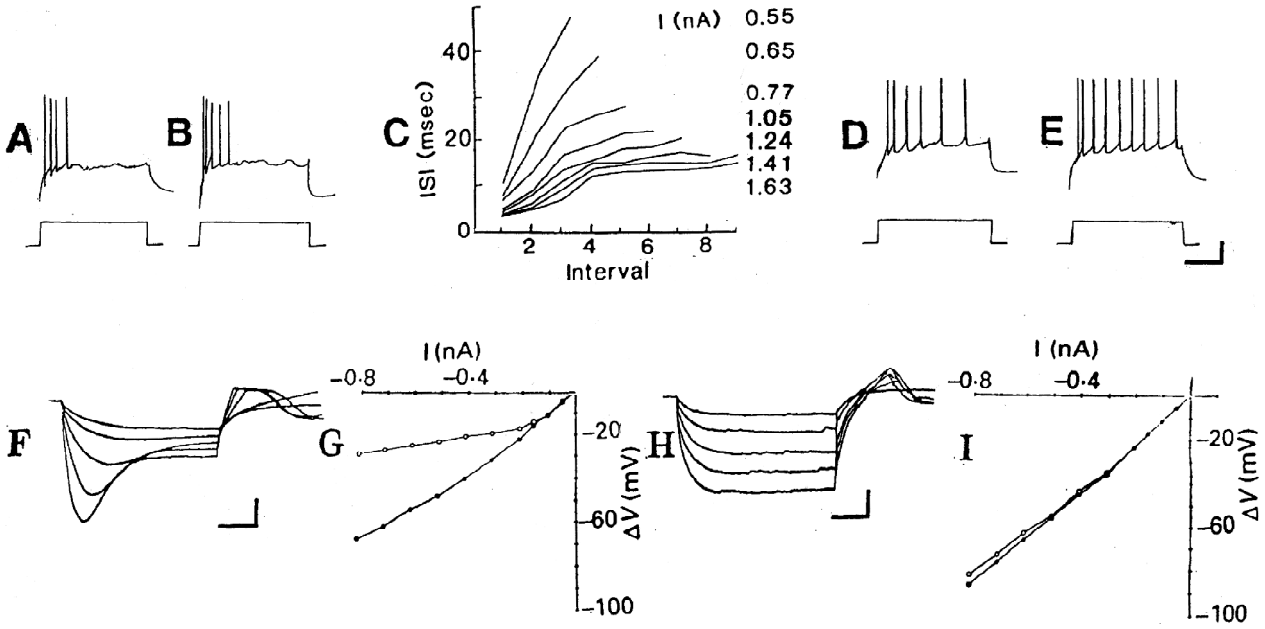

Fig. 2. A-E Response characteristics of CeL output cells to depolarizing current injection A.B. fast adapting cells. C. Graph of interspike interval (lSl) versus interval number for A neuron. Magnitude of injected current for each trace is indicated on the right. D. slow adapting neuron. E. repetitive firing neuron. Calibration: 100 ms. 20 mV. F-I. typical current-voltage relationship (I-V) of two CeL neurons. F and H. Voltage responses to injected hyperpolarizing current pulses (F, -0.1, -0.15, -0.3, -0.5, -0.7 nA; H, -0.1, -0.2, -0.3, -0.4, -0.5 nA). G and I. One curve was obtained by measuring the peak voltage deflection during injection of negative current steps and represents the peak voltage-current relationship(solid circles). The other curve was obtained by measuring the voltage deflection at the apparent steady-state voltage-current relationship.(open circles). Each point is the average of 10 values. Calibration: voltage bar 20 mV. time bar 100 ms.for ABDE and 20ms. For FH. Current intensity 0.8nA

adapting cells, the sustained discharge, evoked by suprathreshold depolarizing current pulses consisted of two or three initial action potentials, with interspike intervals, shorter than those of following action potentials. The doublet or triplet of action potentials was followed by discharge, showing a progressive adaptation in frequency. Fig 2D shows a typical example of slow adapting neuron. This unit fired two spikes at high frequency at the start of current injection and then showed complete spike frequency adaptation. 4 cells fired repetitively with no or small amount of spike frequency adaptation. They generated single spikes during application of depolarizing current pulse (Fig.2E).

The parameters of the current-voltage relationship used in this study were determined from voltage responses to current steps over the range: from resting membrane potential to -90mV. Electrotonic potentials, evoked by injection of transient hyperpolarizing current steps of increasing amplitude had a characteristic shape. In hyperpolarizing potentials a time dependent depolarizing sag was observed between the peak and steady-state amplitude which gradually increased in amplitude, with membrane hyperpolarization [Fig2FH]. In Fig 2GI peak and steady state voltage deflections are plotted as a function of hyperpolarizing current intensity. Current-voltage curves were established for 12 cells. They show that the majority of these cells presented an inward rectification for potentials 10-20 mV more polarized than the resting membrane potential (Fig. 2F-I). No clear correlation was found between the electophysiological classes of cells described above and the characteristics of I-V curves.

Basic membrane properties were studied in 16 units. The input resistance R_N was calculated from the linear portion of the current-voltage plot. The mean values of peak and steady-state input resistances were 29.4$\pm$5 and 19+2.3 MΩ respectively. Mean time constant was 22.2$\pm$3.4 ms. There were no clear differences in the passive membrane properties in cells showing different patterns of firing following depolarizing current injection.

In the present study 12 electrophysiologically characterized neurons were selected for detailed morphological analysis. Neurons were stained with an intracellular injection of biocytin, in order to provide morphological information about the population of units, from which recordings were obtained. Neurobiotin was chosen, because it is stable and does not greatly increase electrode resistance. 9 neurons were successfully injected and were analyzed morphologically in detail. Fig. 3 shows the examples of intracellularly stained CeL efferent neurons, in frontal section. All analyzed neurons were typical "medium spiny neurons". They had fusiform or ovoid pericaria, that averaged 17x13 μm, and 3-5 radially extended primary dendrites, which were moderately spiny, creating a bitufted dendritic pattern. Dendrites usually exhibited 2-3 branch point and extended a total of 150-175 μm. Total dendritic length averaged 2.9-3.5 mm. A rough estimate of the number of spines was made and was an average of 0.2-0.4 dendritic spines per μm of dendritic length, not taking hidden spines into account. In the Table the values of the somatic size, cell volume and the radius of the dendritic domain are listed with electophysiological values.

Although many electophysiological studies on rodent CN neurons have been reported, none have examined the electophysiological properties of cat's CN neurons. Shies et al. [21], using sharp microelectrode recordings from CN neurons, have described two cell types, called type A and B. The properties of these neurons are compatible to those, described here as adapting and repetitive firer cells, respectively. Martina et al. [22] have described three main cell types in CN and called low-threshold bursters, regular spiking and late firing neurons. However, no adapting neurons were described. Employing intracellular recording techniques and subsequent filling with the marker biocytin, it was feasible to

Table

Morphological and electrophysiological properties of identified neurons

	Cell size lxs m	Cell volume m^3	Dendritic radius m	Input resistance megohm	Time constant ms.
1	16x12	1546	160	26	11.23
2	18x13	1702	220	27	9.5
3	19x10	1611	180	29	17.8
4	17x11	1599	200	28	12.0
5	19x14	1621	260	22	9.6
6	18x10	1264	170	32	10.5
7	16x10	1059	185	26	16.5
8	19x16	1861	220	18	13.2
9	18x14	1811	240	33.2	10.6

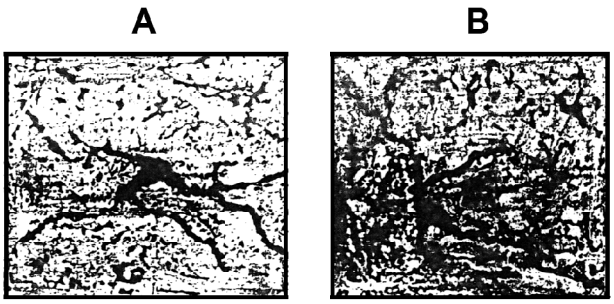

Fig. 3. Photomicrographs of biocytin-stained cat CeL neurons, recovered for morphological analysis in the frontal plane. The length calibration 100 μm.

characterize physiologically and morphologically a population of CeL cells, projected to CeM. The mean findings are as follows: 1. Cells showed firing properties that varied in continuum from those that had marked spike frequency adaptation to cells that fired repetitively with little or no spike frequency adaptation. Hovewer, the most common cell types were those that accommodated fully in response to depolarizing current injection. 2. Examination of the cells and their dendrograms revealed no clear morphological differences between neurons with differing firing properties. 3. There were no clear differences in passive membrane properties, firing threshold and rheobase in cells showing different firing properties. Differences in firing patterns are likely to be determined by different expression patterns of ion channels in neurons. It appears that slow calcium activated potassium currents are key determinants of the repetitive firing properties. They have been proposed to be the major determinants of spike frequency adaptation. Similar regulation of firing patterns has been reported in other structures [23]. The data presented above demonstrated that anatomically identified CeL units projecting to CeM had electrophysiological properties (relative long duration of action potentials, varying degrees of spike frequency adaptation in response to depolarizing current injection) that were generally assumed to be characteristic of projection neurons.

CeL contain a vast array of different neurotransmitters. In CeL neurons neuropeptides are synthetized: enkephalin and corticotrophin-releasing factor. In this structure numerous GABA-ergic interneurones and dophaminergic fibers are described [23] and ionophoretic application of dopamine decreases the spontaneous activity in the CeL neurons. CeL is unique among CN divisions in its extensive connections with different brain structures. Multimodal sensory information as well as information of motivational and emotional relevance converge on the CeL neuron from cortical, amygdaloid thalamic, hypothalamic and brainstem centers. These pecularities indicate that CeL integrates this information to elaborate adequate autonomic and endocrine responses through its extensive efferent pathways with mean output station of the amygdaloid Complex - CeM. CeL has recently attracted considerable attention because of its connections to the basal forebrain, to cholinergic cell rich regions of the sublenticular substantia innominata, the ventromedial globus pallidus and the cellular interstices of the internal capsule [24]. These cholinergic neurons are part of nucleus basalis. The projection of CeL to the cholinergic regions endows it with the potential for widespread influences on the neocortex through modulation of the activity of cholinergic neurons.

ადამიანის და ცხოველთა ფიზიოლოგია

ამიგდალური კომპლექსის ცენტრალური ბირთვის ლატერალური ნაწილის ნეირონთა ელექტროფიზიოლოგიური და მორფოლოგიური თავისებურებანი

გ. თოდუა

პ. ანოხინის სახელობის უმაღლესი ნერვული მოქმედებისა და ნეიროფიზიოლოგიის ინსტიტუტი, რუსეთის მეცნიერებათა აკადემია, მოსკოვი; ი. ბერიტაშვილის სახელობის ფიზიოლოგიის ინსტიტუტი, თბილისი

(წარმოდგენილია აკადემიკოს თ. ონიანის მიერ)

შესწავლილ იქნა ამიგდალური კომპლექსის ცენტრალური ბირთვის ლატერალური ნაწილის ეფერენტულ ნეირონთა ელექტროფიზიოლოგიური და მორფოლოგიური თავისებურებანი. ეფერენტულ ნეირონთა იდენტიფიკაცია ხდებოდა ამავე ბირთვის მედიალური ნაწილის გაღიზიანებაზე მათი ანტიდრომული პასუხების საფუძველზე. გამომყვანი ელექტროდის მეშვეობით დენის გატარებაზე ნეირონთა უმეტესი ნაწილის იმპულსურ აქტიურობას ახასიათებდა მეტ-ნაკლებად გამოხატული ადაპტაცია. ელექტროფიზიოლოგიურად იდენტიფიცირებულ 9 ნეირონში შეყვანილ იქნა ბიოციტინი. როგორც ამ ნეირონთა მორფოლოგიური ანალიზი გვიჩვენებს, ისინი ხასიათდებიან მომრგვალო ან თითისტარისებრი სომით, რომლის ზომაც შეადგენს 18x13,4 მკმ-ს. მათ ახასიათებთ შედარებით ნაკლებად დატოტვილი 3-4 დენდრიტი, საშუალოდ გამოხატული ხორკლიანობით. განიხილება ცენტრალური ბირთვის ლატერალური ნაწილის შესაძლო როლი ამიგდალური კომპლექსის ძირითადი ეფერენტული სტრუქტურის — ცენტრალური ბირთვის მედიალური ნაწილის ფუნქციათა რეალიზაციაში.

REFERENCES

1. *J. Krettek, J.Pare* (1978), J. Comp. Neurol., 178: 255-280.
2. *A. McDonald* (1998), Prog. Brain Res., 55:257-332.
3. *A. Pitkänen* (2000), In: The Amygdala: A Functional Analysis. Oxford Univ. Press.: 31-115.
4. *A. Davis* (1992), In: The Amygdala: Neurobiological Aspects of Emotion, Memory and Mental Disfunction. New York. Wiley-Liss.: 255-33.
5. *J. Le Doux, P. Cichetti, A. Xagoromis* (1990), J. Neurosci., 10:1062-69.
6. *J. Le Doux* (1992), In: The Amygdala: Neurobiological Aspects of Emotion, Memory and Mental Disfunction. New York. Wiley-Liss.: 339-51.
7. *E. Mascagni, A. McDonald, J. Coleman* (1993), Neuroscience, 57: 697-715.
8. *J. Le Doux, C. Farb* (1990), J. Neurosci., 10: 1044-1054.
9. *H. Dong G. Petrowich* (2001), Br. Res., 38: 192-246.
10. *J. Veening, L. Swanson, A. Sawchenko* (1984), Br. Res., 303: 377-57.
11. *M. Behbehani* (1995), Progr. Neurobiol., 46: 575-605.
12. *J. Iwata, J. Le Doux* (1986), Br. Res., 383:195-214.
13. *Y. Smith, D. Pare* (1994), J. Comp. Neurol., 342:232-48.
14. *L. Stefanacci, R. Farb, A. Pitkänen* (1982), J. Comp. Neurol., 323: 586-601.
15. *D. Pare, Y. Smith, J. Pare* (1995), Neuroscience, 69:567-583.
16. *J. Bernard, G. Huang* (1992), J. Neurophysiology, 68:551-560.

17.*L. Freedman, M. Cassel* (1994), Br. Res. 633:243-252.
18.*K. Horikawa, N. Armstrong* (1988), Neurosci. Meth., 25: 1-11.
19.*T. Yamamoto, T. Noda, A. Samejima* (1985), J. Comp. Neurol., 236: 331-347.
20.*H. Jasper, E. Ajmone-Marsan* (1954), Stereotaxic Atlas of Cat's Diencephalons. Ottawa.
21.*M. Shies, P. Callahan* (1999), J. Neurosci. Res., 58: 663-673.
22. *M. Martina, S. Royer, D. Pare* (2003), J. Neurosci., 23: 6876-6883.
23. *D. Madison, R. Nicols* (1984), J. Physiol., 354:1319-1331.
24. *P. Veinante* (1998), BR. Res., 794: 188-198.
25. *B. Kapp, P Whalen* (1994), Behav. Neurosc., 108: 83-93. BB.

Received January, 2010